NONRIGID SINGLE-AXIS SPACE INTEGRATOR DYNAMICS

by

Edward Eugene Shaw

S.B., Massachusetts Institute of Technology
(1960)

SUBMITTED IN PARTIAL FULFILLMENT

OF THE REQUIREMENTS FOR THE

DEGREE OF MASTER OF

SCIENCE

at the

MASSACHUSETTS INSTITUTE OF TECHNOLOGY
May, 1964

Signature of Author Signature redacted
Department of Aeronautics and Astronautics,
May 1964

Certified by Signature redacted
Thesis Supervisor

Certified by Signature redacted
Thesis Supervisor

Accepted by Signature redacted
Chairman, Departmental Committee
on Graduate Students

Thesis
Aero.
1964
M.S.

ACKNOWLEDGMENT

This report was prepared under DSR Project 55-191, sponsored by the Manned Spacecraft Center of the National Aeronautics and Space Administration through Contract NAS 9-153.

NONRIGID SINGLE-AXIS SPACE INTEGRATOR DYNAMICS

by

Edward Eugene Shaw

Submitted to the Department of Aeronautics and Astronautics on 22 May 1964 in partial fulfillment of the requirements for the degree of Master of Science in Aeronautics and Astronautics

ABSTRACT

The general performance equations for a nonrigid single-axis space integrator and a nonrigid single-degree-of-freedom gyroscope are developed to include environmental and nonrigid gyro support effects on instrument dynamics and errors. The performance equations are developed in a matrix form that separates dynamic and excitation terms. Nonrigid single-degree-of-freedom integrating and air bearing gyroscopes and their use in a single-axis space integrator are discussed as special cases of the general performance equations.

Thesis Supervisor: Walter Wrigley, Sc.D.
Title: Professor of Aeronautics and Astronautics

Thesis Supervisor: Robert K. Mueller, Sc.D.
Title: Professor of Aeronautics and Astronautics

ACKNOWLEDGEMENTS

I would like to express my deep appreciation to Professor Walter Wrigley and Professor Robert Mueller for their assistance during all phases of preparing this thesis. Also, my thanks to the Instrumentation Laboratory and, in particular, John Miller and Jim Flanders for their interest in and support of the thesis. Many thanks are due Anthony Moscaritolo for his superb work on all the illustrations.

Finally, my most sincere gratitude to my wife, Beverly, for her typing and assistance in preparing the finished text.

E. E. S.
May 1964

TABLE OF CONTENTS

ILLUSTRATIONS

CHAPTER I

INTRODUCTION

I-A Space Integrator Definition and Function in an Inertial Guidance System

A space integrator is defined as a device which gives a controlled member an angular velocity with respect to inertial space proportional to a command signal even in the face of interferences.[(1),(2)] As used in an inertial navigation or guidance system the space integrator is basically a velocity-controlled servomechanism that matches the inertial angular velocity of its controlled member to a commanded inertial angular velocity. The output of the device may be considered as the orientation of a coordinate frame attached to the controlled member with respect to an inertial coordinate frame and the input as a command inertial angular velocity. In this case the device is performing an integration of the input angular velocity with respect to inertial space. The use of angular velocity in the definition is to avoid the complication involved when using angular displacement, which is not a physical vector quantity. The definition of a space integrator is given mathematically by

$$\overline{W}_{i(cm)} = (PF)_{(si)}\overline{W}_{cmd} \tag{1.1}$$

where:

$\overline{W}_{i(cm)}$ = the angular velocity of the controlled member with respect to inertial space.

$(PF)_{(si)}$ = the performance function of the space integrator.

$\overline{W}_{cmd}$ = the commanded angular velocity of the controlled member with respect to inertial space.

The function of a space integrator in an inertial navigation system is twofold. First it provides isolation of a reference coordinate frame attached to the controlled member from any base motion. Second it rotates the controlled member at an angular velocity with respect to inertial space when commanded to do so by a command input. A special case of the general definition is when the command signal is zero and the controlled member has zero angular velocity with respect to inertial space. This special case implies a stable orientation of the controlled member with respect to inertial space and has given rise to the use of the titles "stable table" and "stable platform" instead of space integrator. These titles suggest the idea that a space integrator stabilizes a coordinate frame with respect to inertial space. This view is often helpful in visualizing the operation of a space integrator.

The single-axis space integrator is a special case of the space integrator discussed and differs only in the respect that it must satisfy the definition about only one axis of the coordinate frame attached to the controlled member. To establish a complete coordinate frame three single-axis space integrators are required. A schematic of a single-axis space integrator is shown in Fig. 1.1 illustrating the major components used in the device.

The function of the components in the system is explained by considering the operation of the single-axis space integrator. A single-degree-of-freedom gyro is used to sense angular velocity with respect to inertial space. The output of the gyro, in the form of an electrical signal, is fed to the servo electronics and amplifier which excites a torque motor whose axis of rotation is the input axis of the gyro. The torque generated by the motor rotates the controlled member at an angular velocity whose sense is opposite to that of the velocity of the base until the input axis of the gyro, mounted on the controlled member, senses no angular velocity with respect to inertial space thus

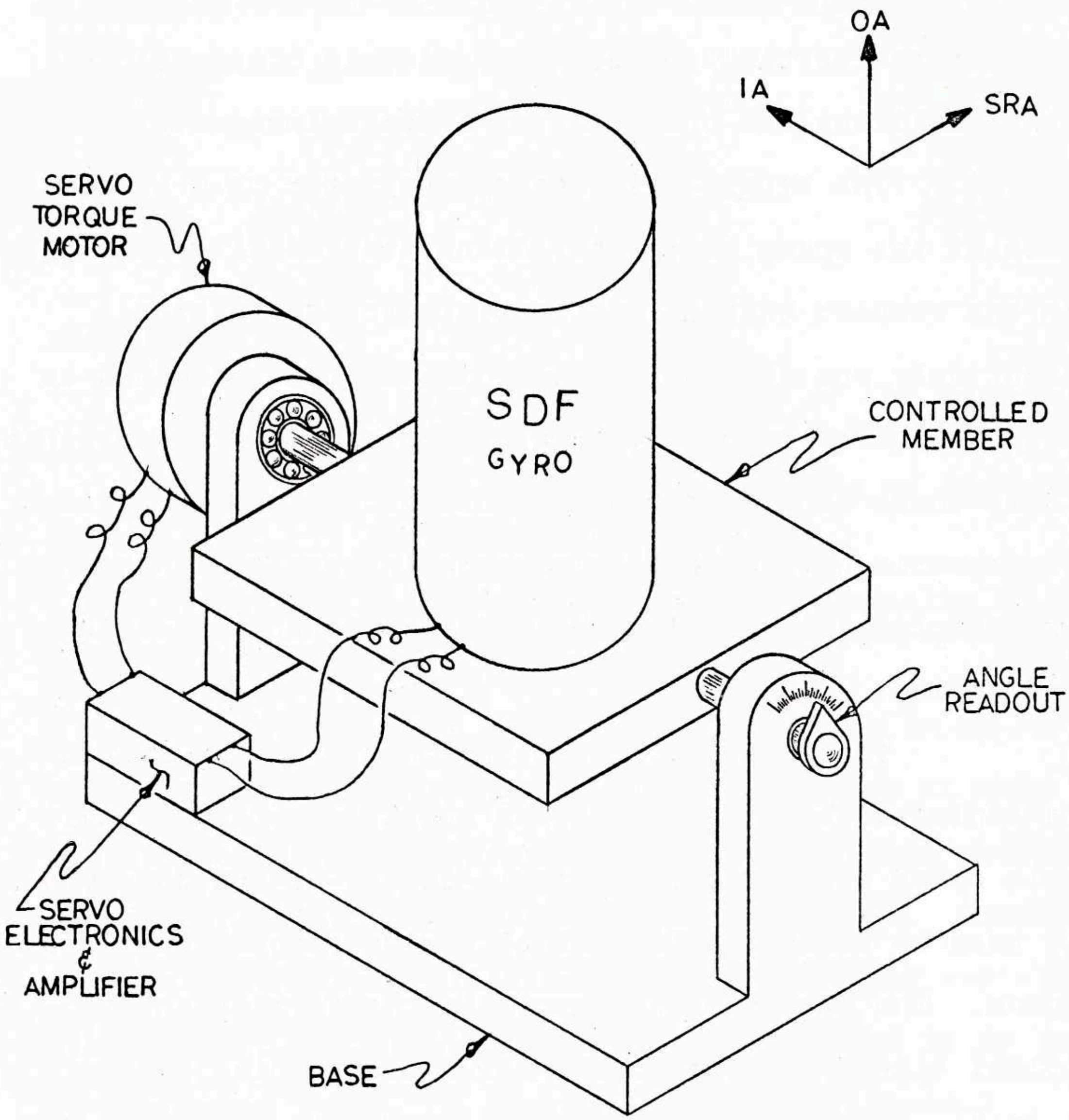

Fig. 1.1 Basic Components of a Single-Axis Space Integrator

stabilizing the controlled direction with respect to inertial space. The developed angle between the controlled member and the base is the integral of the angular velocity with respect to inertial space of the base about the input axis and is the angle that the base has rotated about this axis with respect to inertial space. Fig. 1.2 is a functional block diagram of a single-axis space integrator.

I-B Statement of the Problem

The definition and function of a single-axis space integrator impose the requirement that the angular velocity of the controlled member be proportional only to a command signal. In the mechanization and use of the single-axis space integrator in a guidance system it is necessary to determine if there are any other inputs to the system, and, if other inputs are present, how they affect the performance of the space integrator. The analysis and resultant performance equation must take into account the environment in which the system operates and also the physical properties and construction of the device. For use in a high quality inertial guidance or navigation reference system the output angle of the single-axis space integrator must be accurate to about 20 arc seconds (3)* imposing the

*A representative number used by Wiener in reference 3

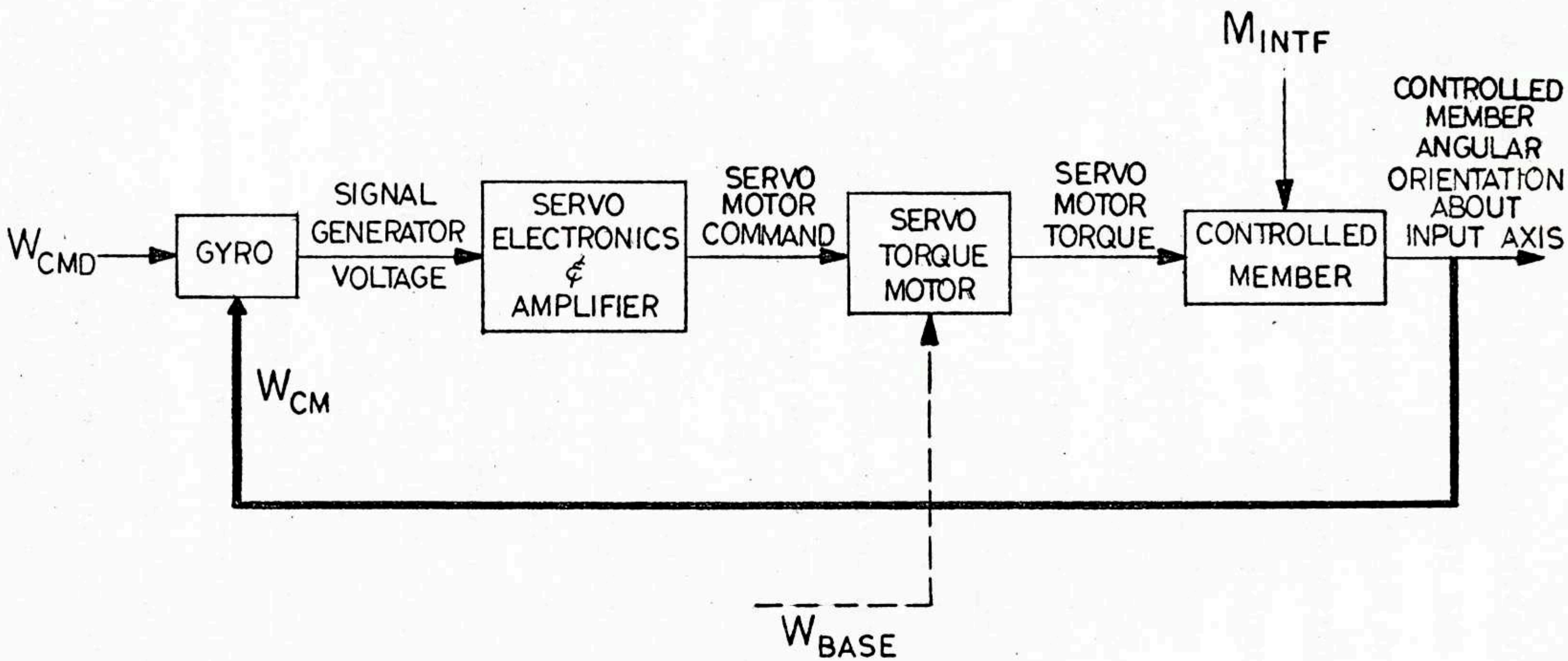

Fig. 1.2 Functional Block Diagram of a Single-Axis Space Integrator

reouirement that the integrated errors due to the environment and properties of the device be either less than 20 arc seconds or be compensated for to this accuracy by a known relationship.

The guidance system in which the single-axis space integrator operates will be mounted in a moving vehicle which is subject to angular velocities about all three axes of a coordinate frame attached to the vehicle. The analysis of the space integrator must then include the effect of angular velocities about all three axes of the coordinate frame attached to the controlled member.

The components of the single-axis space integrator are illustrated in Fig. 1.1. Although all of the components will have nonideal performance, the gyroscope is the prime component that determines the performance function of the single-axis space integrator. The ideal gyro for use in a single-axis space integrator would develop an output angle and electrical signal directly proportional only to an angular velocity about its input axis. In reality the output angle of a gyro is also a function of angular velocities about the spin reference and output axes and mechanical properties of the gyro. For its use in a single-axis space integrator the gyro will be subjected to input angular velocities about all three coordinate axes and the effects of gyro element anisoinertia, nonrigid suspension of the gyro element, compliance of the spin axis bearings, cross coupling of input angular velocities and uncertainty torques as they affect the torques developed about the gyro axes will be considered. The nonrigid support of the gyro element will be examined in detail to determine its effect on the dynamics of the gyro and the associated single-axis space integrator. The integrated errors present in the output angle of the single-axis space integrator as a result of the nonrigid support, coupled with the other conditions imposed on the system, will be examined.

I-C Approach to Problem Solution

The approach to the problem solution will be to first analyze the single-degree-of-freedom gyro subject to the conditions stated in the previous section. The performance equation of the gyro will be written in matrix notation in a form that will separate the dynamics of the gyro from the input excitation terms. This approach illustrates what effects the various conditions have on the gyro performance and permits a more thorough analysis of the effects of nonrigid gyro element suspension on the dynamics of the gyro.

The performance function of the single-axis space integrator will be derived using the matrix notation. The resultant performance function will be in a form that separates the various excitation terms from the dynamics of the single-axis space integrator. The excitation terms can then be analyzed separately to determine their contributions to the resultant error present in the indication of vehicle orientation.

To illustrate the significance and use of the derived performance functions representative cases will be examined for both the gyro and the single-axis space integrator.

I-D <u>Scope of the Investigation</u>

The conditions stated in section I-B for use in this analysis are by no means a complete set of conditions that are present in the single-axis space integrator system. They are, however, the prime conditions that affect the dynamics of the system and include most of the input excitation terms.

A more complete set of conditions would include linear accelerations along all three coordinate frame axes, mass unbalance of the gyro element, anisoelasticity of the gyro element and non ideal performance of the gyro spin motor. These conditions have been analyzed[4] and, with the matrix notation used in the problem solution, these conditions can be analyzed separately and directly inserted into the derived performance equations.

I-E Background and Previous Results

The space integrator, as used in an inertial guidance or navigation system, has been primarily a three, four or five gimballed system that stabilizes a coordinate frame with respect to inertial space. Much analysis work has been done on this type of system, [1], [5], [6], [7], [8] and it is used in most working inertial guidance and navigation systems. The single-axis space integrator has been treated chiefly as a building block toward the understanding and analysis of the three, four and five gimballed system. The analysis of the single-axis space integrator has, therefore, been primarily concerned with special cases that will be helpful in the building block concept. Wrigley[2] has analyzed the single-axis space integrator considering input angular velocities about all three coordinate axes and an elastic support on the gyro input axis. Mueller[9] has analyzed the effect of an elastic input axis support on the dynamics of the output angle of a single-degree-of-freedom gyroscope.

CHAPTER II

SINGLE-DEGREE-OF-FREEDOM GYROSCOPE

II-A Introduction

The single-degree-of-freedom gyroscope has been studied extensively and much literature is available on gyro theory and performance.(1),(2),(4),(9) The purpose of the analysis included in this chapter is not to repeat or add to the previous work but to develop the gyro performance equations in a form and in sufficient detail to make them applicable to the analysis of the single-axis space integrator.

II-B Gyro Model Used for Analysis

Analysis of the gyro will be based on the model illustrated in Fig. 2.1, which shows the nonrigid support of the gyro due to the spin-axis bearings and to the elasticity, radial elastic support and radial damping of the gyro element. These nonrigid support elements develop torques about two axes of the gyro while the torque about the third axis can be developed at the

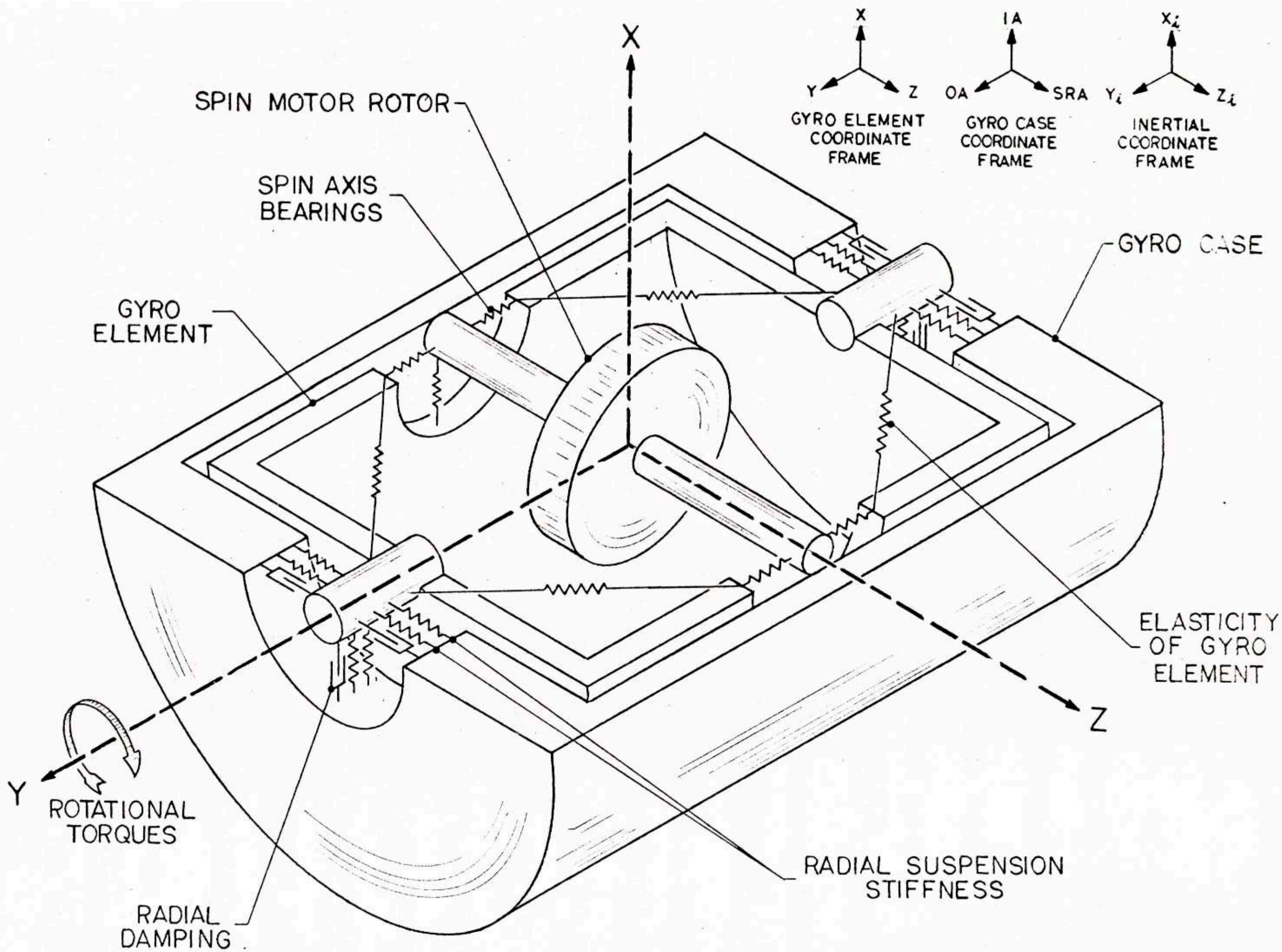

Fig. 2.1 Model of gyro and support system used for analysis

designer's choice to determine the type of single-degree-of-freedom gyro. In section II-D the support system is analyzed in detail.

Three coordinate frames are necessary for a discussion of the nonrigid single-degree-of-freedom gyroscope:

1. inertial frame, i, origin at the center of mass of the earth.
2. gyro case frame, gc, origin at the center of mass of the gyro case, fixed to the gyro case.
3. gyro element frame, ge, origin at the center of mass of the gyro element, fixed to the gyro element.

In a single-degree-of-freedom gyro with a rigid support system the gyro element frame and the gyro case frame would be coincident.

The inertial frame axes will be defined as x_i, y_i, z_i, the gyro case axes as IA, OA, SRA, and the gyro element axes as x, y, and z with their orientation shown in Fig. 2.1.

II-C <u>Derivation of Gyro Element Equation of Motion</u>

The operation of a practical gyroscope is most easily explained by deriving the equations of motion for the gyro element as is done by Wrigley in reference (2). These equations are derived by using Newton's Law for rotation with moments taken about the center of mass of the gyro element.

$$p_i\overline{H}_{ge} = \overline{M} \tag{2.1}$$

where

$p_i\overline{H}_{ge}$ = time rate of change of angular momentum of gyro element with respect to inertial space

$\overline{M}$ = torque applied to gyro element

$p_i \equiv [\frac{d}{dt}]_i$ = time derivative taken in inertial space

$\overline{H}_{ge} = \overline{H}_s + \overline{H}_{ns}$ = angular momentum vector of gyro element

$\overline{H}_s = I_s\overline{W}_s$ = spin angular momentum vector of spin motor rotor

I_s = spin axis moment of inertia of rotor

$\overline{W}_s$ = spin angular velocity vector

$\overline{H}_{ns}$ = non-spin angular momentum vector of gyro element

Applying the law of Coriolis to the left hand side of Eq. (2.1) and separating $\overline{H}_{ge}$ into its spin and non-spin components gives

$$p_i\overline{H}_{ge} = p_{ge}\overline{H}_s + p_{ge}\overline{H}_{ns} + \overline{W}_{i(ge)} \times \overline{H}_s + \overline{W}_{i(ge)} \times \overline{H}_{ns} = \overline{M} \tag{2.2}$$

where $p_{ge} \equiv [\frac{d}{dt}]_{ge}$ = time derivative taken with respect to gyro element

$\overline{W}_{i(ge)}$ = angular velocity vector of gyro element with respect to inertial space.

Assuming W_s = constant(2) the basic law of motion of the gyro element is

$$p_{ge}\overline{H}_{ns} + \overline{W}_{i(ge)} \times \overline{H}_s + \overline{W}_{i(ge)} \times \overline{H}_{ns} = \overline{M} \qquad (2.3)$$

With the gyro element frame oriented as shown in Fig. (2.1) the important quantities in Eq. (2.3) can be written in gyro element axes

$$\overline{W}_{i(ge)} = \overline{i}W_x + \overline{j}W_y + \overline{k}W_z$$

$$\overline{H}_s = \overline{k}I_sW_s$$

$$\overline{H}_{ns} = \overline{i}\ I_xW_x + \overline{j}\ I_yW_y + \overline{k}\ I_zW_z$$

where I_x, I_y and I_z contain both rotor and gyro element inertias about their respective axes. Due to the magnetic coupling between the gyro motor rotor and stator the rotor inertia must be included in I_z. If W_s = constant, as has been assumed, the moment of inertia I_z = constant. Substitution of these quantities into Eq. (2.3) results in a modified Euler equation.

$$I_xpW_x + W_yH_s + (I_z - I_y)W_yW_z = M_x \qquad (2.4a)$$

$$I_ypW_y - W_xH_s + (I_x - I_z)W_xW_z = M_y \qquad (2.4b)$$

$$I_zpW_z + (I_y - I_x)W_xW_y = M_z \qquad (2.4c)$$

The angular motions of interest are those of the gyro element with respect to the gyro case and are shown in Fig. (2.2). With reference to Fig. (2.2) the gyro element coordinate frame is related to the gyro case coordinate frame by an angle transformation matrix. With the assumption that all the angles are

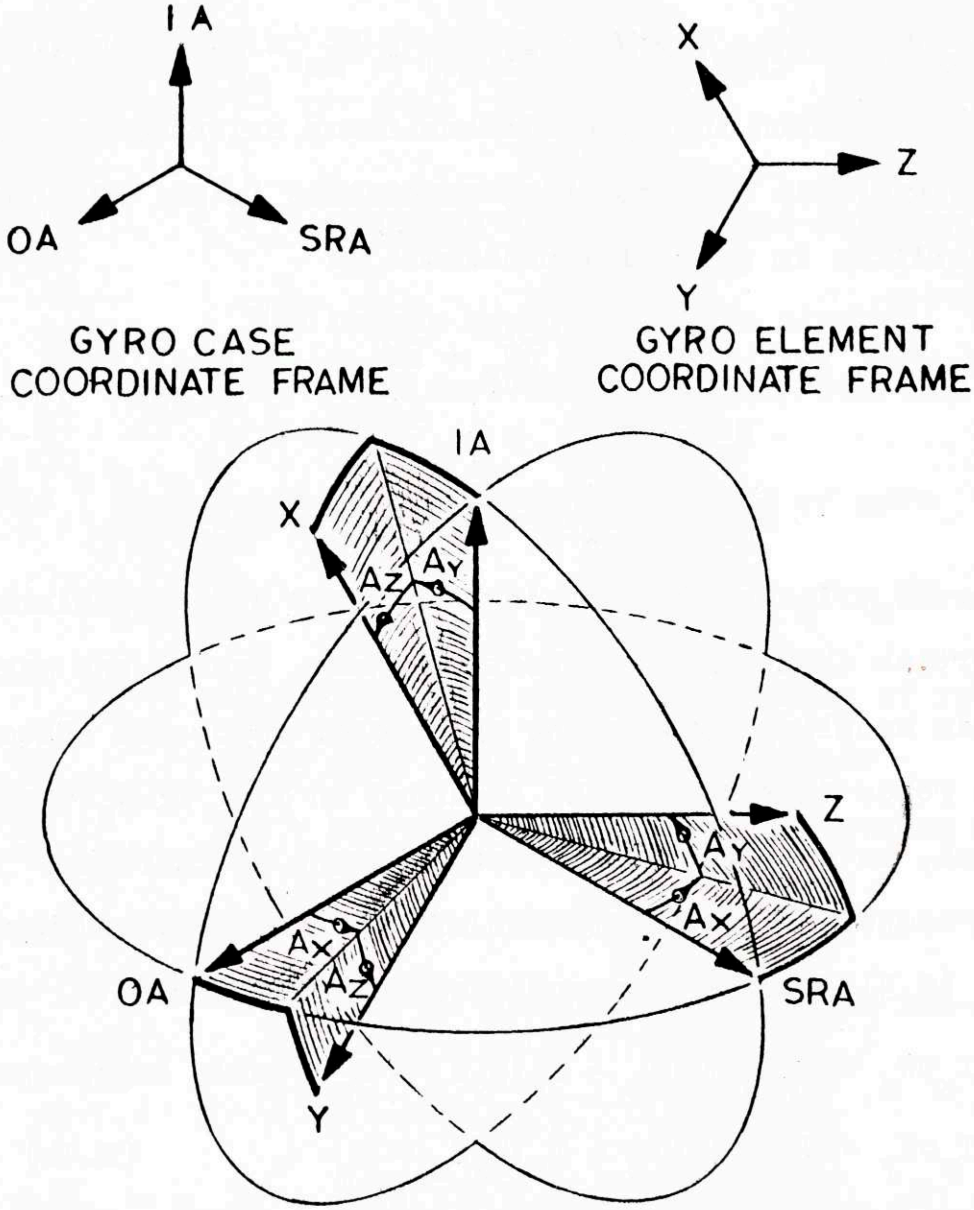

Fig. 2.2 Gyro case and gyro element angular relationship

"small" the transformation matrix $C_{ge}^{gc} = I + A$ where

$$I = \begin{bmatrix} 1 & 0 & 0 \\ 0 & 1 & 0 \\ 0 & 0 & 1 \end{bmatrix} \qquad A = \begin{bmatrix} 0 & A_z & -A_g \\ -A_z & 0 & A_x \\ A_g & -A_x & 0 \end{bmatrix} \tag{2.5}$$

In matrix A the angle A_g is used instead of A_y. This is consistent with common single-degree-of-freedom gyro terminology where the angle about the y-axis is called the gyro angle and labeled A_g.

Using the transformation matrix C_{ge}^{gc} the angular velocities W_x, W_y and W_z can be expressed in terms of W_{IA}, W_{OA} and W_{SRA} and the developed angles A_x, A_g, and A_z as is shown in the matrix Eq. (2.6).

$$\begin{bmatrix} W_x \\ W_y \\ W_z \end{bmatrix} = \begin{bmatrix} 1 & A_z & -A_g \\ -A_z & 1 & A_x \\ A_g & -A_x & 1 \end{bmatrix} \begin{bmatrix} W_{IA} \\ W_{OA} \\ W_{SRA} \end{bmatrix} + \begin{bmatrix} pA_x \\ pA_g \\ pA_z \end{bmatrix} \qquad \begin{matrix} (2.6a) \\ (2.6b) \\ (2.6c) \end{matrix}$$

The equations for W_x, W_y and W_z can now be substituted into Eq. (2.4) to give the equations of motion of the gyro element. Because of the size of the resultant equations they are not written in the text but in section II-E they are written in an equivalent matrix form.

II-D Analysis of Gyro Element Suspension System

The equations of motion of the gyro element have been written in the form of a modified Euler equation where the time derivative of the angular momentum vector with respect to inertial space is equal to the torque applied to the gyro element. It is now necessary to examine how the torques M_x, M_y and M_z are developed in a practical nonrigid gyroscope by using the gyro model of Fig. (2.1).

Fig. (2.1) shows five torques applied to the gyro element. Four of these torques are present due to the nonrigid support of the gyro element while the fifth torque is a rotational torque about the y axis of the gyro element applied at the designer's choice to determine the type of single-degree-of-freedom gyro.

Spin axis bearings behave in an elastic manner when subjected to radial forces.[(2),(9)] As used in the gyro element radial forces are developed along the x and y axes giving rise to torques about the y and x axes respectively.

The gyro element will behave in an elastic manner due to the elastic properties of the element material.[(2),(10)] This elastic behavior will apply torques about the x and z axes.

The support of the gyro element in a single-axis space integrator is either a fluid support or an air bearing type of support coupled with a magnetic suspension support.[10] These supports will apply torques about the x and z axes. In the case of a fluid and magnetic support an elastic behavior will be present due to the magnetic suspension and the forcing of the non-compressible flotation fluid along the y-axis of the gyro element.[11] In addition to the elastic torque a damping torque is present due to the viscous nature of the flotation fluid. In the air bearing and magnetic support an elastic torque is present due to the magnetic suspension and the compressible property of air. In this case the damping torque is essentially zero.

The rotational torque applied to the y-axis of the gyro element determines the type of single-degree-of-freedom gyroscope and may take three forms:

$M_y = -k_g A_g - c_g p A_g$; primarily elastic torque; rate gyro

$M_y = -c_g p A_g$; damping torque; integrating gyro

$M_y = 0$; unrestrained gyro

The torques, M_x, M_y and M_z can now be determined as functions of the gyro suspension system. The analysis of these torques as they apply to the gyro element equations of motion will all take the same form. An equivalent support system model will be defined and a torque angle relationship will be derived in the form $M = kA$ where $k = k(p)$

$\underline{M_x}$

The support system for the x-axis is shown in Fig. (2.3)

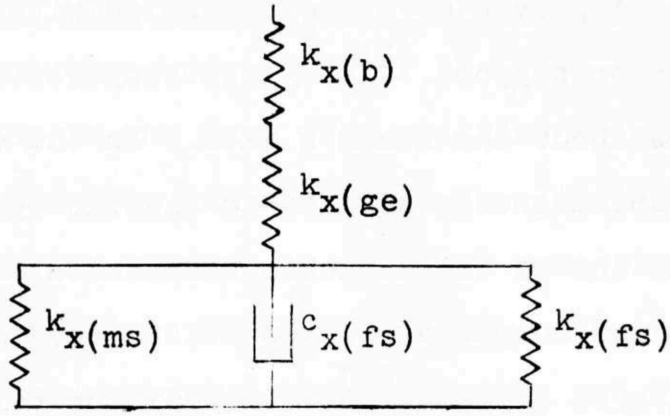

x-Axis support system

Fig.(2.3)

where

$k_{x(b)}$ = elastic coefficient of spin axis bearings

$k_{x(ge)}$ = elastic coefficient of gyro element

$k_{x(ms)}$ = elastic coefficient of magnetic suspension

$k_{x(fs)}$ = elastic coefficient of fluid support

$c_{x(fs)}$ = damping coefficient of fluid support

To simplify the equivalent $k_x(p)$ the spin-axis bearing and gyro element elastic coefficients will be combined in an equivalent $k_{x(ge)(b)}$ where

$$k_{x(ge)b} = \frac{k_{x(b)}k_{x(ge)}}{k_{x(b)}+k_{x(ge)}}$$

In a similar fashion the magnetic and fluid support elastic coefficients will be combined in an equivalent $k_{x(s)}$ where

$k_{x(s)} = k_{x(fs)} + k_{x(ms)}$. The desired k_x is now

$$k_x(p) = \frac{k_{x(ge)(b)}[k_{x(s)} + c_x p]}{k_{x(ge)(b)} + k_{x(s)} + c_x p} \qquad (2.7)$$

Several special cases are of interest when a practical single-degree-of-freedom gyro is considered.

Case A

A single-degree-of-freedom integrating gyro will generally be represented by the special case when

$$k_{x(s)} << k_{x(ge)(b)}$$

$$k_{x(s)} << c_x p$$

$$k_{x(ge)(b)} << c_x p$$

then

$$k_x \cong k_{x(ge)(b)} \qquad (2.7a)$$

A single-degree-of-freedom air bearing gyro could, for different design configurations satisfy any of the three special cases discussed below. In all three cases it is assumed that the stiffness of the spin axis bearing and gyro element, $k_{x(ge)(b)}$, is greater than the suspension stiffness, $k_{x(s)}$, and the radial damping, $c_x p$. With this assumption Case B is satisfied when $k_{x(s)} << c_x p$. Case C is satisfied when $c_x p << k_{x(s)}$ and Case D is satisfied when $k_{x(s)} \cong c_x p$.

Case B

For the special case when

$k_{x(s)} << k_{x(ge)(b)}$

$c_x p << k_{x(ge)(b)}$

$k_{x(s)} << c_x p$

then

$$k_x \cong c_x p \qquad (2.7b)$$

Case C

For the special case when

$c_x p << k_{x(ge)(b)}$

$k_{x(s)} << k_{x(ge)(b)}$

$c_x p << k_{x(s)}$

then

$$k_x \cong k_{x(s)} \qquad (2.7c)$$

Case D

For the special case when

$k_{x(s)} << k_{x(ge)(b)}$

$c_x p << k_{x(ge)(b)}$

$c_x p \cong k_{x(s)}$

then

$$k_x \cong k_s + c_x p \qquad (2.7d)$$

$\underline{M_z}$

The support system for the z-axis is shown in Fig. 2.4.

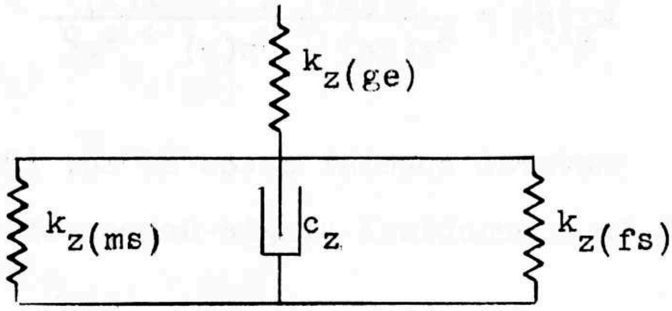

Z-Axis support system

Fig. (2.4)

where:

$k_{z(ge)}$ = elastic coefficient of gyro element about z-axis

$k_{z(fs)}$ = elastic coefficient of fluid or air bearing support about z-axis

$k_{z(ms)}$ = elastic coefficient of magnetic suspension about z-axis

c_z = damping coefficient due to fluid or air bearing support about z-axis

For simplicity in the analysis an elastic coefficient, $k_{z(s)}$, will be defined that combines $k_{z(fs)}$ and $k_{z(ms)}$ where

$$k_{z(s)} = k_{z(fs)} + k_{z(ms)}$$

The equivalent $k_z(p)$ is then:

$$k_z(p) = \frac{k_{z(ge)}[c_z p + k_{z(s)}]}{k_{z(ge)} + k_{z(s)} + c_z p} \qquad (2.8)$$

Several special cases of Eq. (2.8) are of interest in a practical single-degree-of-freedom gyro.

Case A

For the special case when

$$k_{z(s)} << k_{z(ge)}$$

$$k_{z(s)} << c_z p$$

$$k_{z(ge)} << c_z p$$

then

$$k_z \cong k_{z(ge)} \qquad (2.8a)$$

This special case will generally represent most single-degree-of-freedom integrating gyros.

Case B

For the special case when

$$k_{z(s)} << k_{z(ge)}$$

$$k_{z(s)} << c_z p$$

$$c_z p << k_{z(ge)}$$

then

$$k_z \cong c_z p \qquad (2.8b)$$

Case C

For the special case when

$$k_{z(s)} << k_{z(ge)}$$

$$c_z p << k_{z(ge)}$$

$$k_{z(s)} \cong c_z p$$

then

$$k_z \cong k_{z(s)} + c_z p \tag{2.8c}$$

This special case could represent a single-degree-of-freedom airbearing gyro.

M_y

The torque about M_y is the sum of the torque developed due to the elasticity of the spin axis bearings and the designers choice of the type of torque applied about the y-axis. A model of the elements developing this torque is shown in Fig. (2.5).

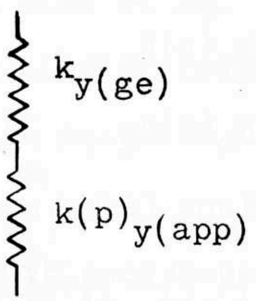

y-Axis torquing elements

Fig. 2.5

where

$k_{y(ge)}$ = elastic coefficient of the gyro spin axis bearings about the y-axis

$k(p)_{y(app)}$ = the applied torque coefficient dependent on the type of applied torque about the y-axis.

The equivalent k_y is then

$$k_y = \frac{k_{y(ge)} k(p)_{y(app)}}{k_{g(ge)} + k(p)_{y(app)}} \tag{2.9}$$

In practical single-degree-of-freedom gyroscopes $k_{y(ge)} >> k(p)_{y(app)}$ and

$$k_y = k(p)_{y(app)} \tag{2.9a}$$

The solution for the equivalent k_x, k_y and k_z torque coefficients makes it possible to write M_x, M_y and M_z in the general form shown in Eq. (2.9)

$$M_x = k_x(p)A_x \tag{2.10a}$$

$$M_y = k_y(p)A_g \tag{2.10b}$$

$$M_z = k_z(p)A_z \tag{2.10c}$$

Equations (2.10) can be substituted into the modified Euler equations of motion of the gyro element to allow a solution that accounts for all of the conditions stated in section I-B.

II-E Matrix Representation of Gyro Equations

The equations of motion of the gyro element obtained when Eq. (2.6) and Eq. (2.10) are substituted in Eq. (2.4) account for all of the conditions stated in section I-B. The three equations resulting from this operation can be linearized and rearranged into the form of Eq. (2.11).

$$a_{11} A_x + a_{12} A_g + a_{13} A_z = b_1 \qquad (2.11a)$$

$$a_{21} A_x + a_{22} A_g + a_{23} A_z = b_2 \qquad (2.11b)$$

$$a_{31} A_x + a_{32} A_g + a_{33} A_z = b_3 \qquad (2.11c)$$

These three equations can be solved simultaneously to find A_x, A_g and A_z. However, the coefficients of Eq. (2.11) contain so many terms that a general solution for A_x, A_g and A_z is not practical and leads to a solution whose complexity tends to mask the physical significance of the conditions imposed on the problem. By rewriting the left hand side of Eq. (2.11) in a matrix form and separating similar terms in the coefficients on both sides it is possible to write Eq. (2.11) in the following form:

$$\left\{\begin{bmatrix} c_{11} & c_{12} & c_{13} \\ c_{21} & c_{22} & c_{23} \\ c_{31} & c_{32} & c_{33} \end{bmatrix} + \begin{bmatrix} d_{11} & d_{12} & d_{13} \\ d_{21} & d_{22} & d_{23} \\ d_{31} & d_{32} & d_{33} \end{bmatrix} + \begin{bmatrix} e_{11} & e_{12} & e_{13} \\ e_{21} & e_{22} & e_{23} \\ e_{31} & e_{32} & e_{33} \end{bmatrix}\right\} \begin{bmatrix} A_x \\ A_g \\ A_z \end{bmatrix} = \begin{bmatrix} f_1 \\ f_2 \\ f_3 \end{bmatrix} + \begin{bmatrix} g_1 \\ g_2 \\ g_3 \end{bmatrix} + \begin{bmatrix} h_1 \\ h_2 \\ h_3 \end{bmatrix}$$

(2.12)

which is the same as

$$(C + D + E)A = F + G + H \tag{2.13}$$

where the matrices are defined as follows

$$C = \begin{bmatrix} \frac{I_x}{k_x} p^2 + 1 & \frac{H_s}{k_x} p & 0 \\ -H_s p & I_y p^2 - k_y & 0 \\ 0 & 0 & \frac{I_z}{k_z} p^2 + 1 \end{bmatrix}$$

where k_x, k_y and k_z are torque coefficients defined in section II-D.

$$D = \begin{bmatrix} \frac{H_s}{k_x} W_{SRA} & -\frac{I_x}{k_x} pW_{SRA} - \frac{I_x}{k_x} W_{SRA}p & \frac{I_x}{k_x} pW_{OA} + \frac{I_x}{k_x} W_{OA}p - \frac{H_s}{k_x} W_{IA} \\ I_y pW_{SRA} + I_y W_{SRA}p & H_s W_{SRA} & -I_y pW_{IA} - I_y W_{IA}p - H_s W_{OA} \\ -\frac{I_z}{k_z} pW_{OA} - \frac{I_z}{k_z} W_{OA}p & \frac{I_z}{k_z} pW_{IA} + \frac{I_z}{k_z} W_{IA}p & 0 \end{bmatrix}$$

$$E = \begin{bmatrix} \frac{(I_z - I_y)}{k_x}(W_{SRA}^2 - W_{OA}^2) & \frac{(I_z - I_y)}{k_x}(W_{OA}W_{IA} + W_{SRA}p) & \frac{(I_z - I_y)}{k_x}(-W_{IA}W_{SRA} + W_{OA}p) \\ (I_x - I_z)(-W_{OA}W_{IA} + W_{SRA}p) & (I_x - I_y)(W_{IA}^2 - W_{SRA}^2) & (I_x - I_y)(W_{OA}W_{SRA} + W_{IA}p) \\ \frac{(I_y - I_x)}{k_z}(W_{SRA}W_{IA} + W_{OA}p) & \frac{(I_y - I_x)}{k_z}(W_{OA}W_{SRA} + W_{IA}p) & \frac{(I_y - I_x)}{k_z}(W_{SRA}^2 - W_{IA}^2) \end{bmatrix}$$

$$F = \begin{bmatrix} -\frac{I_x}{k_x} pW_{IA} - \frac{H_s}{k_x} W_{OA} \\ H_s W_{IA} - I_y pW_{OA} + H_s W_{cmd} \\ -\frac{I_z}{k_z} pW_{SRA} \end{bmatrix}$$

where $H_s W_{cmd}$ is a command torque applied about the y-axis.

$$G = \begin{bmatrix} -\frac{(I_z - I_y)}{k_x} W_{OA} W_{SRA} \\ -(I_x - I_z) W_{IA} W_{SRA} \\ -\frac{(I_y - I_x)}{k_z} W_{OA} W_{IA} \end{bmatrix}$$

$$H = \begin{bmatrix} (U)\ M_x \\ (U)\ M_y \\ (U)\ M_z \end{bmatrix} \qquad A = \begin{bmatrix} A_x \\ A_g \\ A_z \end{bmatrix}$$

Inspection of the defined matrices reveals that each matrix has a physical significance to the conditions imposed on the problem. Matrices C, D and E can be considered as torque coefficient matrices with each matrix having a specific physical significance as listed below.

C - physical properties of a nonrigid single-degree-of-freedom gyro

D - angular velocity and acceleration dependent torque coefficients

E - anisoinertia effects

Matrices F, G and H can be considered as excitation matrices with each matrix having a specific physical significance.

F - Coriolis and angular acceleration excitation torques

G - anisoinertia excitation torques

H - uncertainty torques

Eq. (2.13) can be rearranged as shown in Eq. (2.14)

$$CA = F + G + H - (D + E)A \tag{2.14}$$

where the dynamics of the gyro are on the left side of the equation and on the right side of the equation are excitation terms where $(D + E)A$ is now considered an excitation torque. Another form of Eq. (2.13) can be written as Eq. (2.15)

$$CA + (D + E)A = F + G + H \tag{2.15}$$

In this form the term CA is the primary dynamics of the gyro and $(D + E)A$ is a type of perturbation acting on the dynamics. A complete solution of the problem will give a correct answer for both Eq. (2.14) and Eq, (2.15) but the rearranging illustrates what might be considered as primary and secondary effects.

The matrix representation of the gyro element equations of motion separates the effects of the physical construction of the gyro and the environment in which it operates. This separation makes it possible to analyze each effect separately to determine its contribution to gyro performance.

II-F General Solution of Gyro Equations

Kramer's rule for the solution of simultaneous equations can now be used to solve for A_x, A_g or A_z. When a single-degree-of-freedom gyro is used in a single-axis space integrator the primary angle that must be known explicitly is A_g. The solution for A_x and A_z follows the same pattern as that for A_g.

To solve for A_g the matrix equation in the form of Eq. (2.14) will be used.

$$CA = F + G + H - (D + E)A \tag{2.14}$$

In this form the solution of the determinant of the matrix C represents the dynamics associated with the angle A_g.

$$\left|C\right| = \left(\frac{I_x}{k_x} p^2 + 1\right)\left(I_y p^2 - k_y\right)\left(\frac{I_z}{k_z} p^2 + 1\right) + \frac{H_s^2}{k_x} p^2 + 1) \tag{2.15}$$

A single-degree-of-freedom integrating gyro is generally used in a single-axis space integrator application and at this time it will be assumed that $k_y = -c_g p$. As shown in Appendix A the assumption that $\frac{I_x}{k_x} p^2 \ll 1$ and $\frac{I_z}{k_z} p^2 \ll 1$ is valid over the frequency range of operation of the gyro and will be used at this time. Use of these two assumptions reduces (2.15) to

$$|C| = (I_y + \frac{H_s^2}{k_x}) p^2 + c_g p \qquad (2.16)$$

which is of the same form as that derived in references (2) and (10), with the difference being that k_x is now a general coefficient including all of the assumed nonrigid properties of the gyro. Eq. (2.15) can be written in the form of Eq. (2.17)

$$|C| = c_g p(\frac{I_g}{c_g} p + 1) = c_g p\,(T_g + 1) \qquad (2.17)$$

where

$I_g = I_y + \frac{H_s^2}{k_x}$ = effective output axis moment of inertia

$T_g = I_g/c_g$ = characteristic time of gyro

Using Kramer's rule the general solution of A_g is

$$|C| A_g = \begin{vmatrix} 1 & r & 0 \\ -H_s p & m & 0 \\ 0 & n & 1 \end{vmatrix} \qquad (2.18)$$

where

$$r = f_1 + g_1 + h_1 - A_x(d_{11} + e_{11}) - $$
$$-A_g(d_{12} + e_{12}) - A_z(d_{13} + e_{13})$$

$$m = f_2 + g_2 + h_2 - A_x(d_{21} + e_{21}) - $$
$$-A_g(d_{22} + e_{22}) - A_z(d_{23} + e_{23})$$

$$n = f_3 + g_3 + h_3 - A_x(d_{31} + e_{31}) - $$
$$-A_g(d_{32} + e_{32}) - A_z(d_{33} + e_{33})$$

then

$$\left|C\right| A_g = m + H_s pr \tag{2.19}$$

To illustrate Eq. (2.19) it will be assumed that $A_x << A_g$ and $A_z << A_g$. When the single-degree-of-freedom gyro is used in a single-axis space integrator this assumption may not be valid. The assumption is made here only for the purposes of illustration. Substitution of r and m into Eq. (2.19) gives

$$\left|C\right| A_g = f_2 + g_2 + h_2 + H_s p(f_1 + g_1 + h_1) -$$
$$- A_g(d_{22} + p_{22}) + H_s p[-A_g(d_{12} + e_{12})]$$

Use of the matrix coefficient gives

$$(I_g p^2 + c_g p)A_g = H_s \Big\{ W_{IA} - W_{cmd} - (U)W_y - A_g W_{SRA} - p(U)M_x - $$
$$- \frac{(I_x - I_y)}{H_s} [W_{IA}W_{SRA} + A_g(W_{IA}^2 - W_{SRA}^2)]\Big\} - I_g p W_{OA} \tag{2.20}$$

or

$$(I_g p^2 + c_g p)A_g = H_s\{ \qquad\qquad \} - I_g p W_{OA}$$

Of special interest are two of the special cases for k_x developed in section II-D.

Case A

Case A represents most single-degree-of-freedom integrating gyros with $k_x = k_{x(b)}$. In this case Eq. (2.19) takes the form

$$A_g = \frac{1}{T_g p+1}\left[\frac{H_s}{c_g p}\{ \qquad\qquad \}\right] - T_g W_{OA} \qquad (2.20a)$$

Case B

Case B represents an unrestrained single-degree-of-freedom gyro with $c_g = 0$

$$A_g = \frac{[k_{x(s)}+c_x p]H_s}{[(I_y k_{x(s)}+H_s^2)+I_y c_x p]p^2}\{ \qquad\qquad \} - \frac{1}{p} W_{OA}$$

$$(2.20b)$$

II-G Conclusion

The analysis of a single-degree-of-freedom gyro based on the model illustrated in Fig. 2.1 can be carried out in great detail when a matrix representation of the equations of motion of the gyro element is used. This matrix representation separates the various factors which affect the gyro performance equation making it possible to analyze each term separately.

The representation of a practical single-degree-of-freedom gyro by the model of Fig. 2.1 makes it possible to analyze in detail the effects of a non-rigid support for the gyro element and the equivalent k(p) terms derived in section II-D makes it possible to write one general performance equation for any non-rigid single-degree-of-freedom gyro. Special cases of this general form can then be an integrating gyro, an air bearing gyro or also a rate gyro which was not discussed in this chapter.

II-H Recommendations for Further Study

(1) The model of the gyro in Fig. 2.1 appears to be a representative model for single-degree-of-freedom gyros. However, further study could be done to verify the accuracy and limitations of this representation.

(2) To write the equations of motion of the gyro element in matrix form it was necessary to linearize the equations. Further study could investigate what effects the nonlinear terms have on the gyro performance equations.

(3) With the equations of motion of the gyro element written in matrix form mass unbalance and anisoelasticity of the gyro element in an acceleration field will develop torques about the gyro element axes. These torques can be thought of as excitation terms and they can be analyzed separately using the angle transformation matrix to put the torques into gyro element axes.

The resultant equation can then be directly added to the matrix equation (2.13).

CHAPTER III

NONRIGID SINGLE-AXIS SPACE INTEGRATOR

III-A Introduction

The single-axis space integrator has been defined and its function in an inertial guidance or navigation system has been explained in Chapter I. Section I-B states the conditions imposed on the single-axis space integrator for this analysis and in Section I-C the role of the nonrigid single-degree-of-freedom gyroscope in a single-axis space integrator is explained. In Chapter II the gyro performance equations have been derived and with the matrix representation of these equations used in the derivation of the single-axis space integrator performance equation the effect of the imposed conditions on system performance can be analyzed.

III-B Single-Axis Space Integrator Model Used for Analysis

Fig. 3.1 illustrates the model of the single-axis space integrator that will be used for the analysis. The controlled member is the structure containing the gyro case, the servo torque motor rotor and the connecting shaft between the two. k_x, k_y and k_z are the equivalent torque coefficients derived in section II-D with the factor of 1/4 used only to show the symmetry of the applied torque about the x, y and z axes. It will be assumed that the bearings on the servo drive axis are rigid. The base, as referred to in Fig. 1.1, is now the shell enclosing the gyro and servo drive structure. Damping between the base and controlled member will be considered to be present.

III-C Derivation of Performance Equation

Derivation of the performance equation for the single-axis space integrator is most easily accomplished by considering the controlled member as a torque-summing member and summing all the torques acting on it about IA. These torques are listed below:

$I_{cm}pW_{IA}$ = inertia reaction torque about IA

I_{cm} = moment of inertia of the controlled member about IA

$c_{cm}(W_{IA} - W_b)$ = damping torque about IA

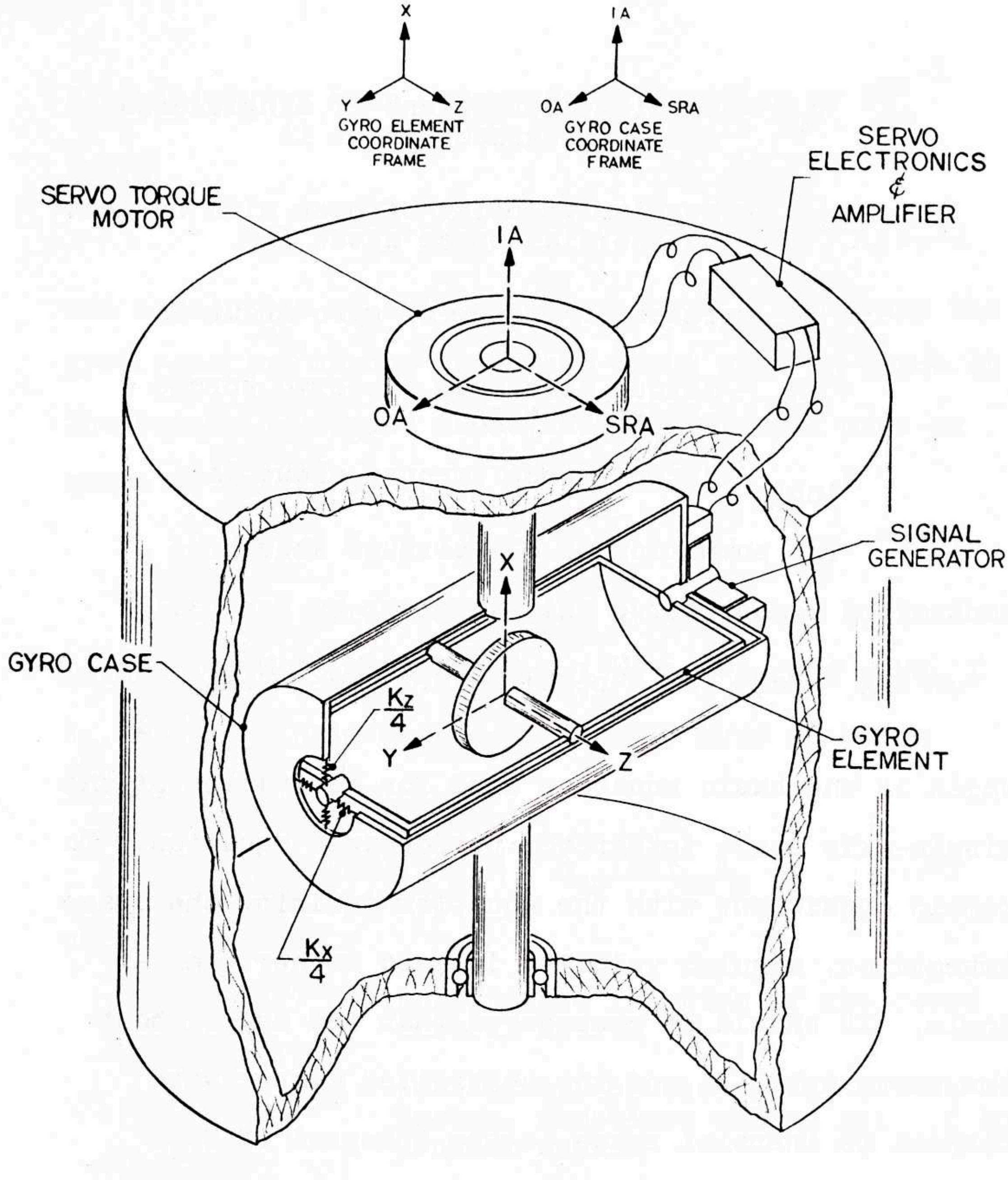

Fig. 3.1 Model of single-axis space integrator used for analysis

c_{cm} = damping coefficient of single-axis space integrator about IA

W_b = angular velocity of base with respect to inertial space about IA

M_r = reaction torque of gyro about IA

M_m = torque developed by servo torque motor about IA

M_{intf} = interference torques about IA

The summation of all torques about the controlled member servo axis is given by Eq. (3.1)

$$I_{cm}pW_{IA} + c_{cm}(W_{IA} - W_{b(IA)}) + M_r = M_m + M_{intf} \tag{3.1}$$

which is the basic equation used for derivation of the single-axis space integrator performance equation. To remain consistent with the equation defining the space integrator, angular velocity is used rather than an angle. It should be remembered that the angle about the servo axis, IA, of the controlled member with respect to inertial space is the integral of W_{IA}.

M_r can be expressed in terms of M_x, M_y and M_z by use of the angle transformation matrix C^{gc}_{ge}. As defined in Chapter II the torque relationship between the gyro element and gyro case coordinate frame is

$$M_{ge} = C^{gc}_{ge} \, M_{gc}$$

Premultiplying both sides of the equation by $C_{ge}^{gc^{-1}}$ gives

$$M_{gc} = C_{ge}^{gc^{-1}} M_{ge} \tag{3.2}$$

and a solution of this equation for M_{IA} expresses the gyro reaction torque about the input axis in terms of the torque developed about the gyro element axes as shown by Eq. (3.3)

$$M_{IA} = M_x + A_z M_y + A_g M_z \tag{3.3}$$

The torque developed by the servo torque motor is directly proportional to the output angle, A_g, of the single-degree-of-freedom gyro as shown in Eq. (3.4).

$$M_m = (PF)_{cs} A_g = - S_{cs} (FF)_{cs} A_g \tag{3.4}$$

where

$(PF)_{cs}$ = performance function of the servo control system

S_{cs} = sensitivity of the servo control system, sometimes called gain of the control system

$(FF)_{cs}$ = frequency function of the servo control system

Substitution of Eq. (3.3) and Eq. (3.4) into Eq. (3.1) gives Eq. (3.5).

$$(I_{cm} p + c_{cm}) W_{IA} = [-S_{cs}(FF)_{cs} + M_z] A_g + c_{cm} W_{b(IA)} - M_x - A_z M_y + M_{intf} \tag{3.5}$$

A solution of the four simultaneous equations, (3.5), (2.11a), (2.11b) and (2.11c) where M_x, M_y and M_z have been replaced by equations (2.10a), (2.10b) and (2.10c) will give the solutions for W_{IA}, A_x, A_g and A_z in a nonrigid single-axis space integrator. The general solution by this method is very tedious, tends to mask the physical significance of the conditions imposed on the problem and involves the simultaneous solution of four nonlinear equations. A useful and accurate solution that eliminates the problem associated with the simultaneous solution is presented in the following section.

III-D Practical Solution of Performance Equation

A practical solution of Eq. (3.5) can be derived by consideration of the basic operation and function of a nonrigid single-axis space integrator. In section I-A the operation of a single-axis space integrator was discussed and it was explained that the function of the single-degree-of-freedom gyro in the single-axis space integrator is as a transducer to sense angular velocity with respect to inertial space, and to transform this angular velocity into a suit-electrical signal that excites a servo drive system. The servo drive system then drives the controlled member, the single-degree-of-freedom gyro case and associated structure, to null the angular velocity about the input axis of the single-degree-of-freedom gyro. The basic operation of a single-axis space integrator is thus dependent mainly upon the gyro output angle, A_g. Because the basic performance equation of the single-axis space integrator is derived by summing torques acting on the controlled member, the terms M_x, M_y and M_z of Eq. (3.5) can be considered as forms of torque interferences acting on the controlled member. With these basic ideas in mind the following approach to the solution of the performance equation of the nonrigid single-axis space integrator is taken.

First, by remembering that Eq. (2.12) is actually representing the torques developed about the x, y and z axes of the gyro element and that due to the nonrigid support of the gyro element these torques can be represented by Eq. (2.9) it is possible to write by inspection of Eq. (2.11) the torques M_x, M_y and M_z. In a single-axis space integrator application M_y and M_z are multiplied by the angles A_z and A_g respectively, per Eq. (3.5), and if, for illustration, higher order terms, A_xA_y , A_x^2, etc., are neglected M_x, M_y and M_z can be written as shown in Eq. (3.6).

$$M_x = I_x p W_{IA} + H_s W_{OA} + (I_x p^2 + H_s W_{SRA}) A_x +$$
$$+ (H_s p - I_x p W_{SRA} - I_x W_{SRA} p) A_g + (I_x p W_{OA} p - H_s W_{IA}) A_z \quad (3.6a)$$

$$M_y = I_y p W_{OA} - H_s W_{IA} - M_{cmd} \quad (3.6b)$$

$$M_z = I_z p W_{SRA} \quad (3.6c)$$

Substitution of Eq. (3.6) into (3.5) gives

$$(I_{cm} p + c_{cm}) W_{IA} = [-S_{cs}(FF)_{cs} + k_g]\, A_g -$$
$$- M_{xx} - M_{xz} - I_x p W_{IA} - H_s W_{OA} + c_{cm} W_b \quad (3.7)$$

where

$$k_g = I_x p W_{SRA} + I_x W_{SRA} p - I_z p W_{SRA} - H_s p$$
$$M_{xx} = (I_x p^2 + H_s W_{SRA}) A_x$$
$$M_{xz} = [I_y p W_{OA} + I_x p W_{OA} p - 2H_s W_{IA} - M_{cmd}] A_z$$

With the performance equation of the single-axis space integrator in the form of Eq. (3.7) the angle A_g for the nonrigid single-degree-of-freedom gyro can be used to find the performance equation of the nonrigid single-axis space integrator. Although it is possible to express a general performance equation for the single-axis space integrator, the more practical approach would be to substitute the performance function of the particular type of single-degree-of-freedom gyro that was to be used in Eq. (3.7). A single-degree-of-freedom integrating gyro and a single-degree-of-freedom air bearing gyro are of particular interest when used in a single-axis space integrator and are discussed below.

III-D.1 Single-Axis Space Integrator Using an Integrating Gyro

A single-degree-of-freedom integrating gyro of the type in Case A of section II-D and Eq. (2-20a), when used in Eq. (3.7), will give the performance function of a nonrigid single axis space integrator as

$$
\begin{aligned}
&[\frac{c_g}{H_s}\frac{I_{cm}}{S_{cs}(FF)_{cs}}(T_g p + 1)p^2 + \frac{c_g}{H_s}\frac{c_{cm}}{S_{cs}(FF)_{cs}}(T_g p + 1)p - \\
&\qquad - \frac{k_g}{S_{cs}(FF)_{cs}} + 1]\, W_{IA} = \\
&[1 - \frac{k_g}{S_{cs}(FF)_{cs}}][W_{cmd} + A_g W_{SRA} - (U)W_y] + \\
&+ [1 - \frac{k_g}{S_{cs}(FF)_{cs}}][\frac{(I_x - I_y)}{H_s}(W_{IA}W_{SRA} + A_g[W_{IA}^2 - W_{SRA}^2])] + \\
&+ [1 - \frac{k_g}{S_{cs}(FF)_{cs}}][\frac{I_g}{H_s}\, pW_{OA}] - \\
&-[\frac{c_g}{H_s}\frac{1}{S_{cs}(FF)_{cs}}(T_g p + 1)p][M_{xx}+M_{xz}+I_x pW_{IA}+H_s W_{OA}-c_{cm}W_{b(IA)}]
\end{aligned}
\qquad (3.8)
$$

The performance equation (3.8) illustrates what parameters effect the dynamics and resulting errors in a nonrigid single-axis space integrator. The parameters

$\frac{c_g}{H_s}$, $\frac{I_{cm}}{S_{cs}(FF)_{cs}}$, $\frac{c_{cm}}{S_{cs}(FF)_{cs}}$, $\frac{k_g}{S_{cs}(FF)_{cs}}$ and T_g are of particular importance. To further analyze Eq. (3.8) the schematic block diagram of the single-axis space integrator, Fig. (3.2), will be used. For illustrative purposes all inputs to the gyro other than $(W_{cmd}-W_{IA})$ will be neglected, it will be assumed that $\frac{k_g}{S_{cs}(FF)_{cs}} \ll 1$ and all interfering torques will be included in M_{intf}. For a complete analysis all of these effects must be included. The output W_{IA} of the system, using an integrating gyro, can now be written as

$$W_{IA} = \frac{\frac{H_s}{c_g}S_{cs}(FF)_{cs}}{p(T_gp+1)(I_{cm}p+c_{cm})+\frac{H_s}{c_g}S_{cs}(FF)_{cs}}\left[W_{cmd}+\frac{c_gp(T_gp+1)}{H_sS_{cs}(FF)_{cs}}pM_{intf}\right]$$

and at the lower frequency end

$$W_{IA} \cong W_{cmd} + \frac{c_g}{H_s}\ \frac{1}{S_{cs}}\ p\ M_{intf}$$

The open loop performance function, $(PF)_{si}$

$$(PF)_{si} = \frac{S_{cs}(FF)_{cs}}{c_{cm}}\ \frac{H_s}{c_g}\ \frac{1}{p(T_gp + 1)(T_{cm}p + 1)}$$

$$\text{where } T_{cm} = \frac{I_{cm}}{c_{cm}}$$

For a single-axis space integrator to be accurate to 0.1 meru, the error introduced by pM_{intf}, the servo gain, S_{cs}, must be adjusted accordingly. To illustrate

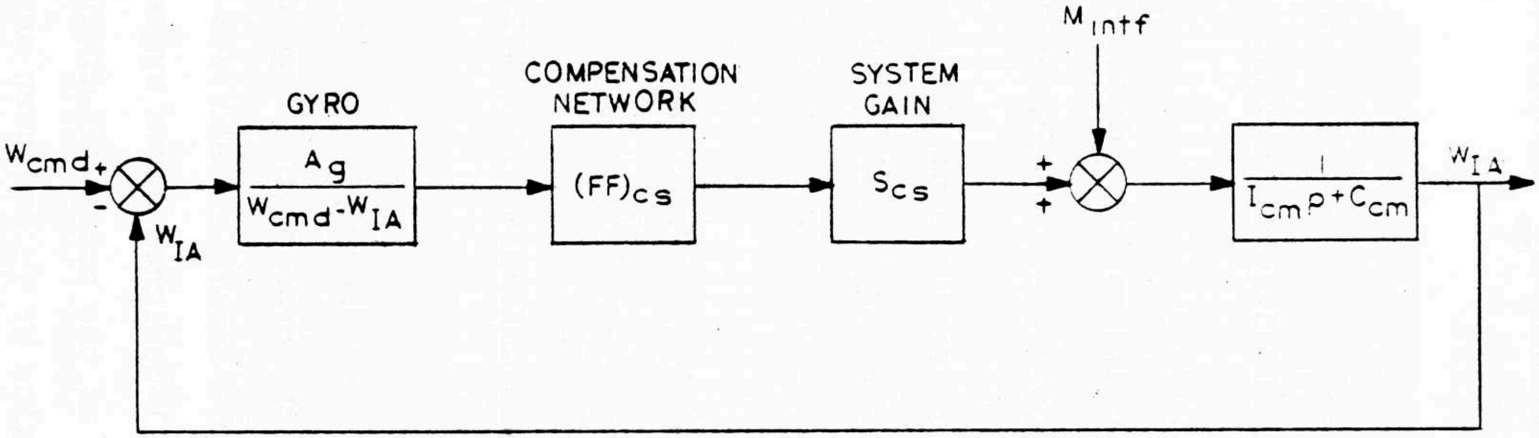

Fig. 3.2 Schematic block diagram for single-axis space integrator

the method of calculating S_{cs} the following parameters will be chosen

$$\frac{H_s}{c_g} = 1$$

$$c_{cm} = 10.000 \text{ dyne cm/rad/sec.}$$

$$T_{cm} = 0.05 \text{ sec.}$$

$$T_g = 0.0017 \text{ sec (calculated } \frac{I_y}{c_{g_I}} \text{ for a HIG-4 gyro)}$$

$$T_g = 0.0027 \text{ sec (experimental } \frac{I_g}{c_g} \text{ for a HIG-4 gyro)}$$

The two values of T_g are used to illustrate the effect of nonrigidity on the single-axis space integrator operation. For $W_{IA} = 0.1$ meru due to $pM_{intf} = 1{,}000$ dyne cm/sec

$$S_{cs} = 10^{11} \text{ dyne cm/rad and}$$

$$G = \frac{S_{cs}}{c_{cm}} \frac{H_s}{c_g} = 10^7$$

With $S_{cs} = 10^{11}$ dyne cm/rad the assumption $\frac{k_g}{S_{cs}} << 1$ is valid.

Fig. 3.3 is a Bode plot of $(PF)_{si}$ for both values of T_g. At the crossover frequency, 0db, the phase shift is -207° for $T_g = .0027$ sec and 200° for $T_g = .0017$. A well-designed servo system has about -135° phase shift at the crossover frequency and, if the theoretical value of T_g had been used for servo compensation, a phase shift of 65° would stabilize the servo system. Due to the nonrigid support system in the gyro the compensation network must provide an

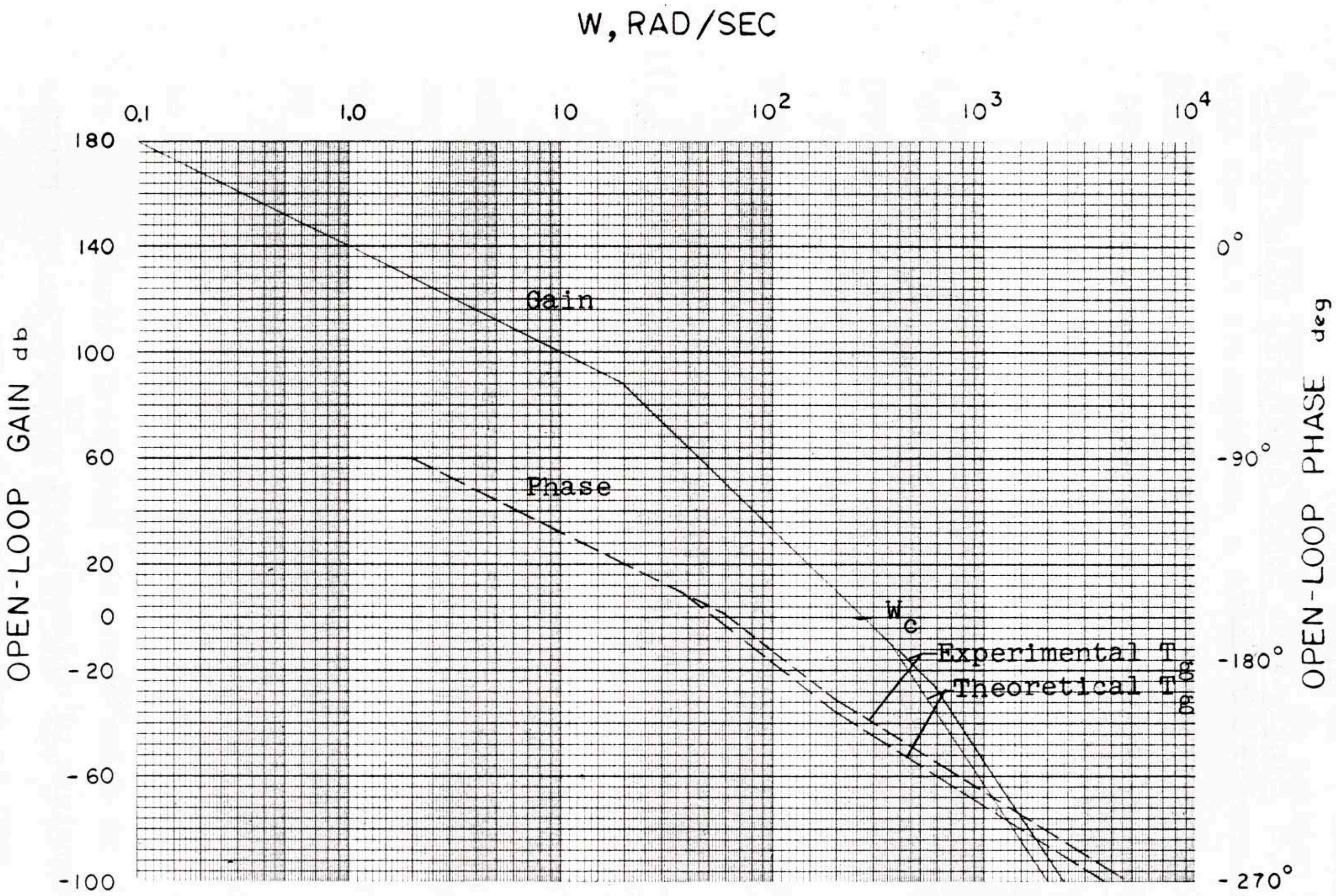

Fig. 3.3 Open-loop transfer function for a single-axis space integrator utilizing an integrating gyro

additional 7° of phase shift.

III - D.2 Single-Axis Space Integrator Using an Air Bearing Gyro

A single-degree-of-freedom gyro of the type in Case D of section II-D and Eq. (2.20b), when used in Eq. (3.7), will give the performance function of the single-axis space integrator as

$$\left[\frac{I_{cm}}{S_{cs}(FF)_{cs}} \frac{I_{ga}}{H_s} (1+b\,T_{ga}p)p^3 + \frac{c_{cm}}{S_{cs}(FF)_{cs}} \frac{I_{ga}}{H_s}(1+bT_{ga}p)p^2 + \right.$$
$$\left. + (1+T_{ga}p)\left(1 - \frac{k_g}{S_{cs}(FF)_{cs}}\right)\right] W_{IA} =$$

$$= \left[1 - \frac{k_g}{S_{cs}(FF)_{cs}}\right][1 + T_{ga}p][W_{cmd} + A_g W_{SRA} - (U)W_y] +$$
$$+\left[1-\frac{k_g}{S_{cs}(FF)_{cs}}\right][1+T_{ga}p]\left[\frac{(I_x-I_y)}{H_s}(W_{IA}W_{SRA}+A_g[W_{IA}^2-W_{SRA}^2])\right] +$$
$$+\left[1 - \frac{k_g}{S_{cs}(FF)_{cs}}\right][1 + T_{ga}p]\left[\frac{I_{ga}}{H_s} \frac{1}{p} W_{OA}\right] -$$
$$- \frac{I_{ga}}{H_s} \frac{(1+bT_{ga}p)p^2}{S_{cs}(FF)_{cs}}[M_{xx}+M_{xz}+I_x pW_{IA}+H_s W_{OA}-c_{cm}W_{bIA}] \tag{3.9}$$

where $$I_{ga} = I_y + \frac{H_s^2}{k_{x(s)}}$$

$$T_{ga} = \frac{c_x}{k_{x(s)}}$$

$$b = \frac{I_y}{I_{ga}}$$

The parameters of interest are $\frac{I_{cm}}{S_{cs}(FF)_{cs}}$, $\frac{c_{cm}}{S_{cs}(FF)_{cs}}$, $\frac{k_g}{S_{cs}(FF)_{cs}}$, $\frac{I_{ga}}{H_s}$, T_{ga} and b. Using Fig. (3.2) and following the same procedure as used in section III-D.1, with the same assumptions, a single-axis space integrator using an air bearing gyro can be analyzed as shown below.

For the low frequency region

$$W_{IA} \cong W_{cmd} + \frac{I_{ga}}{H_s S_{cs}} p^2 M_{intf}$$

The open loop transfer function is

$$(PF)_{si} = \frac{H_s(S_{cs})(FF)_{cs}}{I_{ga} c_{cm}} \frac{[1 + T_{ga} p]}{p^2[1+bT_{ga}p][T_{cm}p+1]}$$

To solve for I_{ga} assume, as reasonable engineering values,

$$I_y = 35 \text{ gm cm}^2$$

$$H_s = 10^4 \text{ gm cm}^2/\text{sec}$$

$$k_x(s) = 5 \times 10^5 \text{ dyne cm/rad}$$

which gives $I_{ga} = 235$ gm cm^2 and $b = 0.15$

For $p^2 M_{intf} = 500$ dyne cm/sec^2 and $c_{cm} = 10^4$ dyne cm/rad/sec. the gain $S_{cs} = 10^9$ dyne cm/rad for a 0.1 meru uncertainty due to $p^2 M_{intf}$.

Fig. 3.4 is a Bode plot of $(PF)_{si}$, subject to the above conditions, for $c_x = 0$ and $T_{cm} = 0.05$ sec. At the crossover frequency the phase shift is -235° which requires a phase shift of 100° for a well designed servo system. Fig. 3.5 is a Bode plot of $(PF)_{si}$ for $T_{ga} = 0.01$ sec. At the crossover frequency the phase shift is 212° which requires a phase shift of 77° for a well designed servo system.

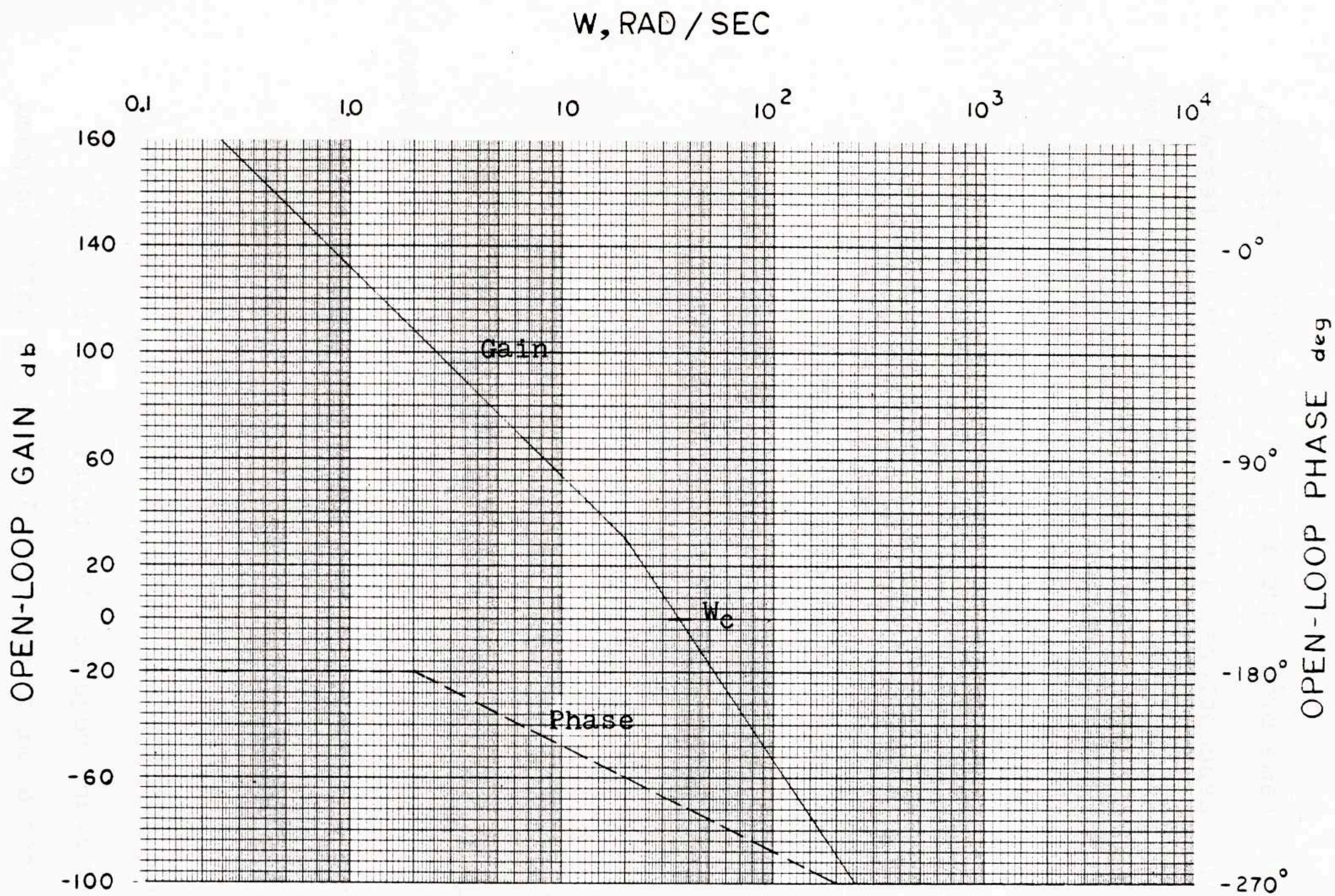

Fig. 3.4 Open-loop transfer function for a single-axis space integrator utilizing an air bearing gyro with no radial damping

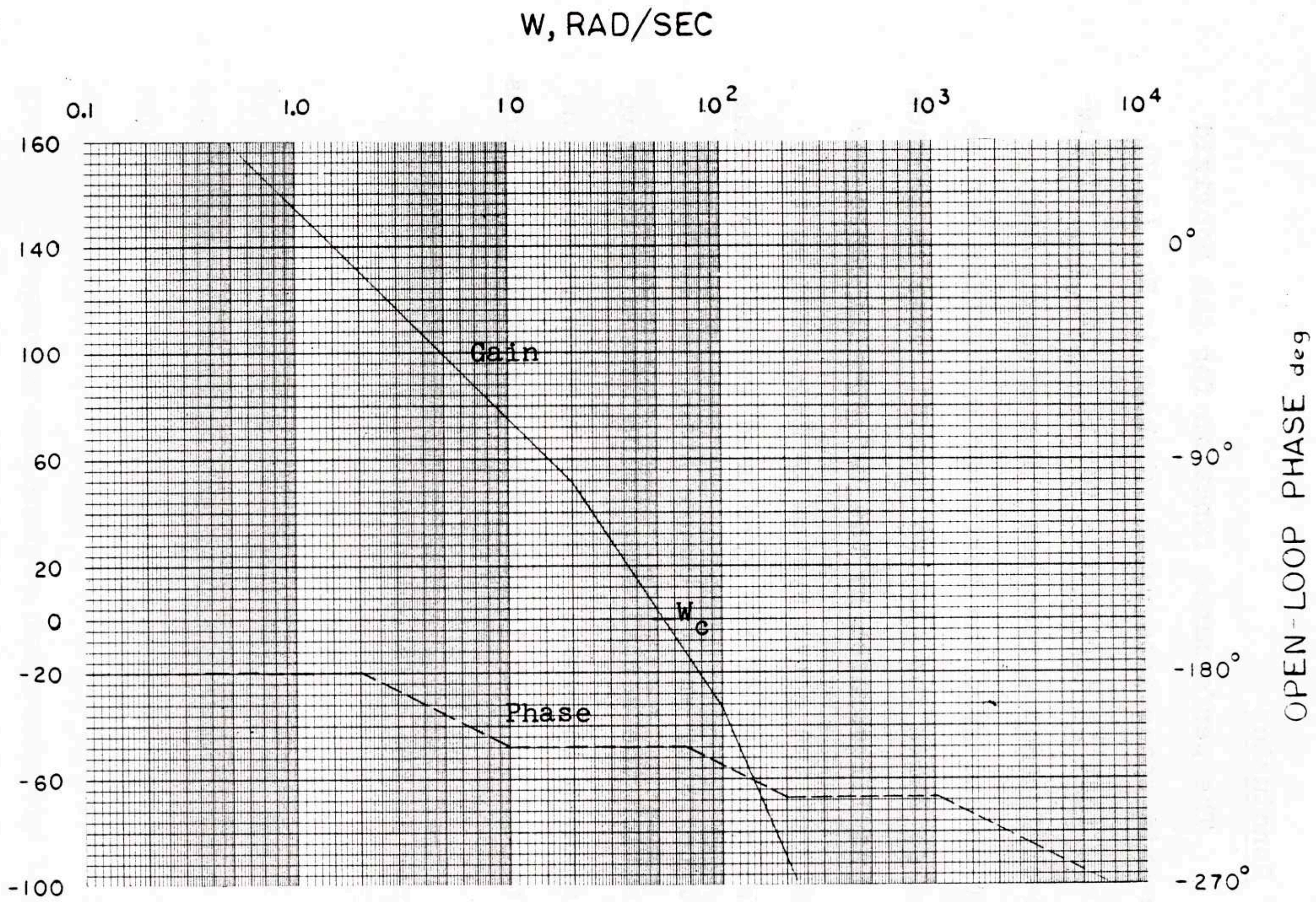

Fig. 3.5 Open-loop transfer function for a single-axis space integrator utilizing an air bearing gyro with radial damping

III-E Conclusion

The performance function for the nonrigid single-axis space integrator is shown in Eq. (3.7) in a form that is applicable for use with all single-degree-of-freedom gyroscopes. For a particular appliation and gyro the performance function can be derived as shown for the two special cases in section III-D. As illustrated by the two special cases the stability of the servo system is dependent on the suspension system of the gyro used in the single-axis space integrator and to insure stability by servo compensation the actual suspension system of the gyro must be known in detail. When a mission velocity and acceleration profile is specified the excitation terms in Eq. (3.7) can be analyzed in detail to determine the error in the axis orientation.

CHAPTER IV

SUMMARY OF RESULTS AND CONCLUSION

The general performance equation for a nonrigid single-axis space integrator, as shown in Fig. 3.1, is given by Eq. (3.7)

$$(I_{cm}p + c_{cm})W_{IA} = [-S_{cs}(FF)_{cs} + k_g]A_g -$$
$$-M_{xx} - M_{xz} - I_x p W_{IA} - H_x W_{OA} + c_{cm}W_b \qquad (3.7)$$

This form of the equation includes all of the conditions imposed on the device in section I-B while retaining the physical significance of the conditions and allows the designer of a single-axis space integrator to separate and analyze independently the effect of the various conditions on the dynamics and accuracy of the device.

The development in Chapter II of the performance equations of the nonrigid single-degree-of-freedom gyro allows the designer of a single-axis space integrator or a single-degree-of-freedom gyro to include the effects of a nonrigid gyro element support in his analysis and to analyze the gyro in as much detail as he desires by separately analyzing the contributions of the imposed conditions. When the performance equations for the gyro have been developed, including as many conditions as is desired, they may be substituted into the general single-axis space integrator equation, Eq. (3.7), and the single-axis space integrator can then be analyzed in as much detail as is desired.

A step-by-step analysis of a single-axis space integrator would proceed as follows:

1) Determine type of single-degree-of-freedom gyro to be used in the single-axis space integrator.
2) Determine the physical parameters of the gyro including the type of gyro element suspension that is present.
3) Using section II-D determine the equivalent k_x, k_y and k_z that represent the gyro element suspension.
4) Using Eq. (2.11) write the gyro equations in a matrix form, this can generally be done by inspection of the gyro coefficient matrices that are defined.

5) Decide what terms should be included in the gyro performance equations.
6) Following the procedure of section II-F, determine the gyro performance equations.
7) Use the gyro performance equations in Eq. (3.7) to determine the single-axis space integrator performance equation.
8) Select a representative mission velocity and acceleration profile.
9) Analyze the single-axis space integrator performance equation to determine the requirements of the control system performance function to achieve the desired system accuracy.
10) Perform an error analysis on the system to determine the effects of the terms not included in the first analysis.

The following conclusions can be stated as a result of the analyses carried out in Chapters II and III.

1) A general set of performance equations can be written for a nonrigid single-degree-of-freedom gyro including all effects of environment and physical construction in a matrix form that separates the various conditions.
2) An equivalent suspension system can be derived for any nonrigid single-degree-of freedom gyro. (Note that the suspension stiffness used in the performance equations is general and that even if a suspension system other than that shown in Fig. 2.1 is present the derived performance equations are still valid.)

3) The dynamics of a single-degree-of-freedom gyro are independent of the z-axis suspension system when $\frac{I_z}{k_z} p^2 \ll 1$. For a practical single-degree-of-freedom integrating gyro this assumption is valid.

4) A general performance equation for a nonrigid single-axis space integrator can be derived that includes all effects of environment and physical construction in a form that separates the effects of the various conditions.

5) The dynamics of the single-axis space integrator are dependent on the nonrigid suspension system in the gyro as illustrated in section III-D. To insure servo stability for the single-axis space integrator the gyro suspension system must be known in detail.

CHAPTER V

RECOMMENDATIONS FOR FURTHER STUDY

As a result of the analysis and matrix representation of the gyro performance equation in Chapter II the following recommendations for further study are suggested.

1) Representation of other Gyro Performance Parameters in Matrix Form

With the matrix form of the gyro element equations of motion, Eq. (2.11), other parameters that affect gyro operation can be derived, written in a matrix form and directly added to Eq. (2.11). These parameters might include mass unbalance, anisoelasticity, etc.

2) Analysis of a Single-Degree-of-Freedom Gyro used in a "Strapdown" System

The equations developed in Chapter II for a nonrigid single-degree-of-freedom gyro lend themselves directly to the analysis of a gyro where a loop is closed about the signal generator and torque generator. An analysis following the approach of Chapter II where $k_y = kA_g$ will yield the performance of the gyro in a "strapdown" system.

3) Analysis of a Pendulous Integrating Gyro Accelerometer

The pendulous integrating gyro accelerometer (PIGA) can be analyzed using the same approach that was used for the analysis of the single-axis space integrator. Eq. (3.7) for the single-axis space integrator is also applicable for the PIGA and when Eq. (2.11) includes the effect of an introduced mass unbalance, pendulosity, about the y-axis of the gyro element the performance equation for the PIGA can be obtained. The derived equation will be subject to the same conditions that are present in the single-axis space integrator analysis.

Appendix A

ANALYSIS OF GYRO SUSPENSION STIFFNESSES

Draper et al[1] have presented experimental and theoretical data for a particular HIG-4 gyro. Wrigley[2] has used these data to calculate $k_x = 5 \times 10^6$ dyne cm/rad and an undamped natural frequency of 50 cps to verify the assumption that $\frac{I_x}{k_x} p^2 \ll 1$.

To verify $\frac{I_z}{k_z} p^2 \ll 1$ assume

(1) $I_x = I_z$

(2) $k_{x(ge)} = k_{z(ge)} = k_z$

where

$k_{x(ge)}$ = elastic stiffness of the gyro element about the x axis

$k_{z(ge)}$ = elastic stiffness of the gyro element about the z axis

k_z = total elastic stiffness about the z axis; see section II-D.

For $k_x = k_{x(ge)(b)} = \dfrac{k_{x(ge)}k_{x(b)}}{k_{x(ge)} + k_{x(b)}}$

where

$k_{x(b)}$ = elastic stiffness of the spin axis bearings about the x axis

assume, as reasonable engineering values, that

(1) $k_{x(ge)} = \frac{1}{10} k_{x(b)}$

(2) $k_{x(ge)} = k_{x(b)}$

(3) $k_{x(ge)} = 10\, k_{x(b)}$

For these values the undamped natural frequency about the z axis is 53 cps, 70 cps and 165 cps respectively to verify the assumption that $\frac{I_z}{k_z} p^2 << 1$.

REFERENCES

1. Draper, C.S., Wrigley, W. and Grohe, L.R., The Floated Integrating Gyro and Its Applications to Geometrical Stabilization Problems of Moving Bases, S.M.F. Fund Paper FF-13, New York, Institute of the Aeronautical Sciences, 1955.

2. Wrigley, W., Single-Degree-of-Freedom Gyroscopes, presented at IUTAM Symposium on Gyrodynamics, Celerina, Switzerland, M.I.T. Instrumentation Laboratory Report R-375, Cambridge, Mass., 1962.

3. Wiener, T.F., Theoretical Analysis of Gimballess Inertial Reference Equipment Using Delta-Modulated Instruments, M.I.T. Sc.D. Thesis, Department of Aeronautics and Astronautics, M.I.T. Instrumentation Laboratory Report T-300, Cambridge, Mass., 1962.

4. Weinstock, H., The Effects of Vibration on Gyroscope Instruments, M.I.T. Instrumentation Laboratory Engineering Memo E-1399, Cambridge, Mass., 1963.

5. Stockard, J.L., Space Integrator Dynamics, M.I.T. Sc.D. Thesis, Department of Aeronautics and Astronautics, Cambridge, Mass. 1961.

6. Broxmeyer, C., Inertial Navigation Systems, Chapter 4, New York, McGraw Hill Book Company, 1964.

7. Hovorka, J., Dynamics of the Gyro-Stabilized Platform, M.I.T. Instrumentation Laboratory Report R-403, Cambridge, Mass., 1963.

8. Draper, C.S., Wrigley, W. and Hovorka, J., Inertial Guidance, Chapter 7, New York, Pergamon Press, 1960.

9. Mueller, R.K., Proposed Method for Producing a Lead Performance Function in Integrating Gyros, M.I.T. Instrumentation Laboratory Engineering Note E-38, Cambridge, Mass., 1951.

10. Gilinson, P.J., Jr., Denhard, W.G. and Frazier, R.H., A Magnetic Support for Floated Inertial Instruments, S.M.F. Fund Paper FF-27, New York, Institute of the Aerospace Sciences, 1960.

11. Draper, C.S., Finston, M., Denhard, W.G. and Goldenberg, D., Dynamic Support of Instrument Components by Viscous Fluids, Proceedings of the First International Congress of the International Federation of Automatic Control, Moscow, Russia, 1960, reprinted from Automatic and Remote Control, Butterworths, London, 1960.